Chalcogenide Letters Vol. 14, No. 11, November 2017, p. 489 - 497

PHYSICO-CHEMICAL PROPERTIES OF THE $Ge_8Sb_{2-x}Bi_xTe_{11}$ BULKS AND THIN FILMS

V. KARABYN[a*], D. HIMICS[a], J. PRIKRYL[b], L. BENES[a], R. SVOBODA[d], B. FRUMAROVA[c], T. WAGNER[a], M. FRUMAR[a]

[a] *Department of General and Inorganic Chemistry, Faculty of Chemical Technology, University of Pardubice, Studentska 95, 532 10 Pardubice, Czech Republic*

[b] *Center of Materials and Nanotechnologies, Faculty of Chemical Technology, University of Pardubice, Nam.Cs. Legi 565, CZ-530 02, Czech Republic.*

[c] *Institute of Macromolecular Chemistry of Czech Academy of Sciences, v.v.i., Heyrovskeho nam. 2, 162 06 Prague, Czech Republic*

[d] *Department of Physical Chemistry, Faculty of Chemical Technology, University of Pardubice, Studentska 573, 532 10 Pardubice, Czech Republic*

In this work the structure, thermal, electrical and optical properties of $Ge_8Sb_{2-x}Bi_xTe_{11}$ (x = 0; 1; 2) thin films were investigated. Thin films were prepared by Flash Thermal Evaporation (FE) and by Pulsed Laser Deposition (PLD) techniques. The amorphous structure of all as-deposited films were proofed by X-ray diffraction analysis. All samples crystallize in the structure of cubic rock salt with a space group Fm−3m after the heat treatment. The crystallization behavior of $Ge_8Sb_{2-x}Bi_xTe_{11}$ thin films were studied by the thermal analysis. It was found that the substitution of Sb by Bi leads to the decrease of the crystallization temperature and activation energy of the studied samples. The electrical sheet resistance R_s of as-deposited thin films, measured by the four probe method according to van der Pauw showed that the difference in R_s values between the amorphous and crystalline states decreases by around 4 orders of magnitude. The refractive index was increasing with the increase of Bi concentration related with the higher polarizability of Bi in comparison with Sb. The optical contrast for studied materials were determined from reflectivity and it was found to be more than 20 %.

(Received August 2, 2017; Accepted November 24, 2017)

Keywords: PCM; thin films; flash thermal evaporation; pulsed laser deposition; GST; Amorphous materials; crystalline.

1. Introduction

Phase-change memory (PCM) materials are widely used for optical data storage and now are finding application in the electronic non-volatile memory (NVM) devices, but the structure of the phases involved and the nature of the phase transition in the nanoscale bits pose continuing challenges. Optical data storage products have been used, such as compact discs (CD), digital versatile discs (DVD), high-definition digital versatile discs (HD DVD), Blu-ray discs (BD) [1, 2]. Initially, the main problem with PCM technology was related to the instability of devices because of spontaneous crystallization. This was the starting point of massive research of materials along the pseudo-binary GeTe-Sb_2Te_3 tie-line [3-16].

Currently, one of the prime candidates for PCM materials is represented by Ge-Sb-Te (GST) thin films, which has great technological importance for the data storage devices, [17, 18]. GST materials used in optical or electrical storages can be reversibly switched between amorphous and crystalline state which is accompanied by the high contrast in the optical reflectivity and electrical conductivity. Using X-ray diffraction it was observed that GST compounds crystallize

[*]Corresponding author : vasyl.karabyn@student.upce.cz

into cubic rock-salt like structure [2]. Subsequent Extended X-ray Absorption Fine Structure (EXAFS) [19-22] studies performed on crystalline GST was found that the bond lengths are equal to sum of covalent radii of particular elements and the main structural units are $GeTe_4$ tetrahedrons and $GeTe_3$ and $SbTe_3$ pyramids. Furthermore was showed that the octahedral units are locally distorted, i.e. there are two subsets of bond lengths 3 shorter and 3 longer [23]. It is important to note that bond lengths are longer in both cases in comparison with counterparts observed in the amorphous state. From one perspective the formation of so-called “resonance bonding” in the crystalline phase [24, 25] is the main cause of drastic changes in the optical and electrical properties of amorphous and crystalline phases, but from other opinion showed that was not found any change in optical transition, which is necessary to support the idea of resonance bonds [26].

$Ge_2Sb_2Te_5$ has been singled out as a prototypical material which has been commercialized in the data storage media [2]. Recently, it was found that GeTe-rich alloys such as $Ge_8Sb_2Te_{11}$ possesses larger optical contrast at the wavelength of 405 nm which is used in the Blu-ray technology [27, 28]. One of the possible ways how to improve the material properties lies in the doping of the pseudo-binary GST compound with other elements that shows severe alteration of the properties [21, 22, 29]. Demand on increasing of the speed and density of the recording process led to a consideration of Bi as one of potential elements for substitution of Sb by Bi. It is in the same group as Sb but possesses a larger atomic radius [9]. The study of the behavior of GST materials doped with the Bi has been reported in the literature [30, 31] where it was shown that the substitution of Sb by Bi lowers the crystallization temperature and activation energy. Thereby, Bi can be considered as curious element for substitution of the GST materials. Therefore, the aim of this work was to study the structure, thermal, electrical and optical properties of the GST materials, where Sb was substituted by Bi in the compositional series $Ge_8Sb_{2-x}Bi_xTe_{11}$ (where x = 0; 1; 2).

2. Experimental

The $Ge_8Sb_{2-x}Bi_xTe_{11}$ (where x=0; 1; 2) alloys were prepared by the melt-quenching technique from high-purity (5N) elements (Ge, Sb, Bi, Te). The amount of each element in appropriate composition was calculated according to their atomic percentage and then sealed in quartz ampoules in a vacuum of $1\cdot10^{-3}$ Pa. The materials were heated in steps up to 980 °C. Each synthesis was continued for 24 hours at the maximum temperature in a rocking furnace. After heating, the quartz ampoules were quenched in cold water to prevent composition separation from occurring. From these alloys thin films were prepared by two deposition techniques: Flash Thermal Evaporation (FE) [32] and Pulsed Laser Deposition (PLD) [33, 34].

Amorphous thin films with composition of $Ge_8Sb_{2-x}Bi_xTe_{11}$ and a thickness of ≈200 nm were prepared by the Flash Thermal Evaporation (FE) on glassy substrate in the chamber with pressure of $2\cdot10^{-4}$ *Pa.* The deposition rate was 0.3 nm/s.

The Pulsed Laser Deposition (PLD) technique was also used for the preparation of amorphous thin films with the thickness of ≈200 nm. PLD technique with a KrF excimer laser (λ = 248 nm) was used with the following parameters: a pulse duration of 30 ns, repetition rate of 20 Hz, energy fluence on the target of ~2.6 $J\cdot cm^{-2}$.The amorphous thin films were deposited in a vacuum chamber (background pressure of ~$3\cdot10^{-4}$ Pa). The substrates were rotated in an off-axis geometry to improve the thickness homogeneity of the films.

Crystalline thin films were prepared by annealing procedure at temperatures that were 20°C higher than the crystallization temperature of amorphous phase T_c, for 30 min in Argon atmosphere.

The structure of the amorphous and crystalline thin films was studied by X-ray diffraction (XRD) analysis, employing a diffractometer Bruker AXS, D8-Advance using the Cu*Kα* radiation with a secondary graphite monochromator. The measurement was carried out from 10° to 80° with 0.02° step.

The chemical composition of prepared samples was verified by the energy dispersive X-ray (EDX) microanalyzer IXRF System with a GRESHAM Sirius 10 detector and a scanning electron microscope JEOL JSM-5500LV.

The chemical composition of prepared samples was verified by the electron microscope JEOL JSM-5500LV with energy-dispersive X-ray (EDX) microanalyzer (IXRF Systems, detector GRESHAM Sirius 10).

Thermal properties of FE as-deposited thin films were measured using differential scanning calorimetry (DSC) with a Perkin-Elmer Pyris 1 device. The thin films were scraped off the glass substrate and sealed into aluminium pans. Measured data from an empty capsule was subtracted from the data measured with the sample. The measurements were carried out at temperatures from 25 °C to 300 °C using the heating rates of 5, 10, 20, 40 and 80 °C/min. The crystallization temperature, Tc was determined from the maximum of crystallization peaks on the obtained DSC curves. The activation energy of crystallisation E_{ac} of prepared thin films was evaluated using Kissinger's plot [35]. The Kisssinger equation is given by

$$ln(\beta/T_c^2) = C - (E_a/RT_c) \quad (1)$$

where β is the heating rate, T_c is crystallisation temperature, C is a constant, E_a is the activation energy of crystallization and R is the gas constant.

The electrical sheet resistance, R_s of as-deposited thin films was measured by the four-probe method according to van der Pauw [36] under vacuum with a heating rate of 2 *°C/min*.
The optical constants (*n, k*) were calculated using the variable angle spectroscopic ellipsometry (VASE®, J. A. Woollam Co., Inc.). The data was recorded in the spectral region of 300-2300 nm with the step of 20 nm and angles of incidence of 65°, 70° and 75°, respectively. These constants were parameterized by Gaussians and Tauc-Lorentz oscillators [37].

Spectral dependence of optical reflectivity was measured using double-beam UV/Vis/NIR spectrophotometer (JASCO V-570) in the spectral region from 300 to 2000 nm. Aluminium film was used as reference sample for optical reflectivity measurement.

3. Results and discussion

XRD analysis of bulk samples confirmed that all materials contain crystalline cubic Fm-3m structure with lattice parameter (Tab. 1). The corresponding Miller indices and the calculated peak position for the patterns are listed in Table 1. A slight increase in the lattice parameter of cubic structure is observed with increasing the amount of Bi for the bulk samples However, in the case of $Ge_8SbBiTe_{11}$ bulk samples the rhombohedral R-3m phase was observed as well. On the contrary, the $Ge_8Bi_2Te_{11}$ bulk samples contain P-3m1 hexagonal phase together with Fm-3m cubic phase (Fig.1). Formation of the rhombohedral and hexagonal phases may be due to the emergence of Bi_2Te_3, as described in the literatures [38, 39].

Table 1. Results of the lattice parameters (a, c) for bulk samples with composition of $Ge_8Sb_2Te_{11}$, $Ge_8SbBiTe_{11}$, $Ge_8Bi_2Te_{11}$ at room temperature

Bulk	Crystalline phases	cubic	hexagonal	
		a (Å)	*a* (Å)	*c* (Å)
$Ge_8Sb_2Te_{11}$	Ge8Sb2Te10 cubic Fm−3m (225)	5.980	-	-
$Ge_8SbBiTe_{11}$	Ge6.04Sb2.68Te10 cubic Fm−3m (225)	5.996	4.383	16.105
	Ge7.8Bi1.3Te10 cubic Fm−3m (225)			
	GeBi2Te4 rhombo. H. axes R3m (166)			
$Ge_8Bi_2Te_{11}$	Ge7.8Bi1.3Te10 cubic Fm−3m (225)	6.005	4.289	17.327
	Ge0.992Te cubic Fm−3m (225)			
	Ge1.5Bi2.5Te5 hexagonal P−3m1 (164)			

The amorphous character of all as-deposited samples prepared by PLD and FE was confirmed by the XRD patterns. After annealing processes at appropriate temperatures (Fig. 1), peaks appear in the XRD patterns, indicating that during the annealing process, there is a transition from the amorphous to the crystalline phase of the thin films prepared by PLD and FE, with the presence of cubic phases in all cases. In the case of the $Ge_8Sb_2Te_{11}$ and $Ge_2Bi_2Te_{11}$ thin film materials prepared using the PLD technique, were used the higher temperature 220 and 180 °C for the annealing process comparatively with the thin films prepared by FE, because the low temperature (180 and 140 °C) was not enough for crystallization of thin films, that may be due to the higher density of films prepared by PLD in comparison with FE [33, 40, 41].

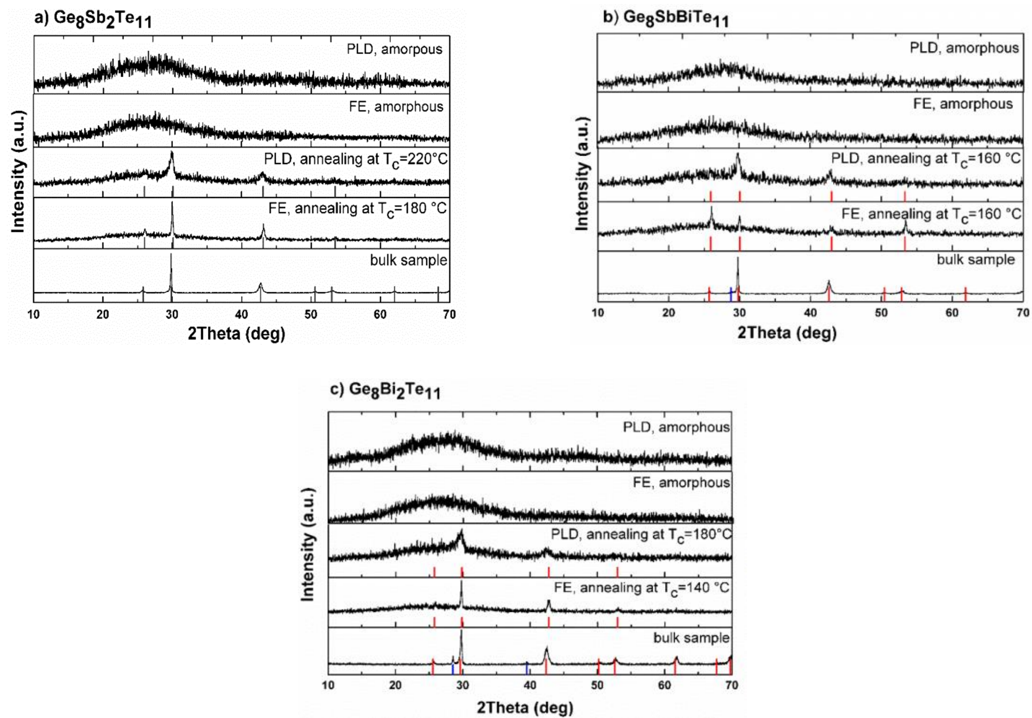

Fig. 1. X-ray diffractograms of the bulk sample, as-deposited and annealed thin films of the a) $Ge_8Sb_2Te_{11}$ b) $Ge_8SbBiTe_{11}$ c) $Ge_8Bi_2Te_{11}$ composition. The positions of diffraction peaks are denoted with vertical bars (red: cubic phase, blue: hexagonal phase).

The composition of $Ge_8Sb_{2-x}Bi_xTe_{11}$ thin films was also investigated by EDX spectroscopy. The obtained results were then compared with the bulk composition for every composition (Table 2). We noted that the error limit of the used EDX method was ± 2 at. %. From the EDX results it can be seen that there is slight deviation between the thin films and bulk compositions. This may be due to the prepared process of thin films that passes at high temperature.

Table 2. Energy-dispersive X-ray spectroscopy of studied thin films in at.%.

Sample	Technique / Element	EDX		Bulk composition	Difference	
		FE	PLD		FE	PLD
$Ge_8Bi_2Te_{11}$	Ge (at.%.)	37.44	40.5	38.1	-0.66	2.41
	Bi (at.%.)	9.09	12.5	9.52	-0.43	2.97
	Te (at.%.)	53.47	50,3	52.38	1.09	-2.08
$Ge_8SbBiTe_{11}$	Ge (at.%.)	39.38	38.3	38.1	1.28	0.2
	Sb (at.%.)	3.39	3.5	4.76	-1.36	-1.26
	Bi (at.%.)	5.1	5.69	4.76	0.34	0.93
	Te (at.%.)	52.13	49.45	52.38	-0.25	-2.93
$Ge_8Sb_2Te_{11}$	Ge (at.%.)	39.43	40.05	38.1	1.33	1.95
	Sb (at.%.)	8.63	9.43	9.52	-0.89	-0.1
	Te (at.%.)	49.93	48.52	52.38	-2.45	-3.86

Generally the crystallization temperature (T_c) and the activation energy of crystallization (E_{ac}) of a phase change material are used as the first indication of its archival life stability. DSC curves of the $Ge_8Sb_{2-x}Bi_xTe_{11}$ thin films measured at temperatures up to 300 °C are shown in Fig.

2a. One can observe the well-defined exothermic peaks corresponding to the crystallization process. The crystallization temperatures (T_c), are summarized in Table 3. The crystallization temperature decreased with the increasing of Bi content. The activation energy was determined by the Kissinger's method [35] from the crystallization temperature and the heating rate. The Kissinger plot of $ln(\beta/T_c^2)$ vs. $10^3/T_c$ for $Ge_8Sb_{2-x}Bi_xTe_{11}$ thin films are shown in Fig. 2b. Each plot exhibited a straight line giving a good correlation coefficient (R). The values of R were close to 1 in almost all cases, which indicated that the Kissinger method [35] can be applied for the determination of the activation energy of the crystallization (E_{ac}) process. Calculated E_{ac} values decrease with increasing Bi content in GST films. This decrease can be explained either by the difference of the crystalline phases which were formed for every composition, or due to the change of structure ordering that occurred at the new phase change switching mechanism as reported in previous work [42].

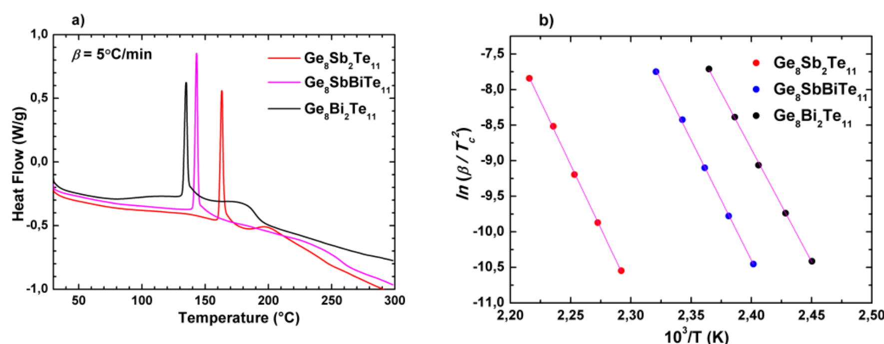

Fig.2 a) DSC scans of as-deposited thin films with 5 °C/min (β) heating rate, b) plot of $ln(\beta/T_c^2)$ vs. $10^3/T_c$ for $Ge_8Sb_{2-x}Bi_xTe_{11}$ thin films.

Table 3. The crystallization temperature T_c, enthalpy ΔH, activation energy of crystallization E_{ac} of the $Ge_8Sb_{2-x}Bi_xTe_{11}$ system from differential scanning calorimetry with 5 °C/min heating rate

System	Method	DSC		
		T_c (°C)	E_{ac} (kJ/mol)	ΔH (meV/at)
$Ge_8Sb_2Te_{11}$	FE	163	296.9	-49.1±3.1
	PLD	-	-	-
$Ge_8SbBiTe_{11}$	FE	143	280.9	-39,4±3,7
	PLD	-	-	-
$Ge_8Bi_2Te_{11}$	FE	135	263.4	-51.3±3.3
	PLD	-	-	-

In Fig. 3, the sheet resistance (R_s) variations of the amorphous $Ge_8Sb_{2-x}Bi_xTe_{11}$ thin films upon heating and cooling process with a heating rate of 2 °C/min. are presented in the temperature range of 25 – 300 °C. From this picture it is seen that the value of R_s was around 10^7 – 10^9 Ω/sqr. for thin films at room temperature. With temperature increase up to 300 °C was observed decrease in R_s values to a final value of 10^2 Ω/sqr., that was specified in paper [36]. At the temperatures from the room temperature to T_g, the temperature dependence of the R_s are consistent with Arrhenius relation [43]. The sheet resistance of $Ge_8Sb_{2-x}Bi_xTe_{11}$ thin films decreases drastically around at 150 °C, that can be explain by the structural transformation of the film. The steep drop in R_s value 3 – 4 orders of magnitude at the transition temperature is due to the phase transformation from amorphous to crystalline phase, the R_s values then continue to decrease gradually. In addition, it can be observed that in the crystalline region during the cooling stage from 300 °C to room temperature the resistance (R_s) for thin films $Ge_8Sb_{2-x}Bi_xTe_{11}$ (x =0, 1 and 2), are almost

constant, that is a characteristic of degenerative semiconductors, but for the thin films prepared by PLD the sheet resistance (R_s) values partially increases, that indicating the semiconductor properties [44].

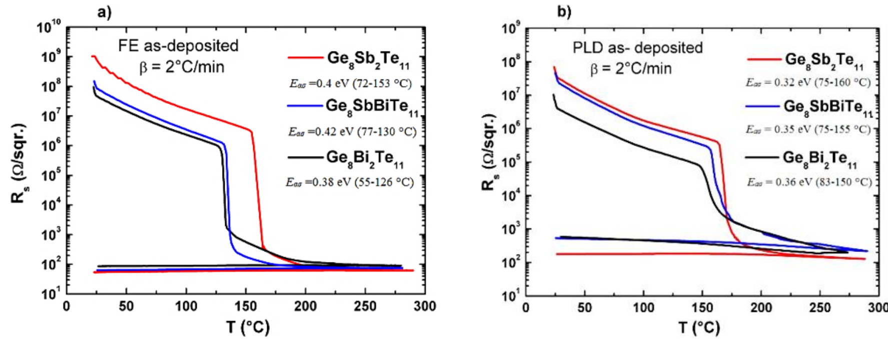

Fig. 3. Isokinetic temperature dependence of electrical sheet resistance R_s of $Ge_8Sb_{2-x}Bi_xTe_{11}$ thin films prepared by a) flash thermal evaporation and by b) pulsed laser deposition, β is heating rate. The activation energies of electrical conductivity $E_{a\sigma}$ and transition temperature T_g, of the amorphous $Ge_8Sb_{2-x}Bi_xTe_{11}$ thin films at 2 °C/min heating rate.

Variable angle spectroscopic ellipsometry (VASE) was used for the determination of the refractive index (*n*), extinction coefficient (*k*) and the thicknesses of the deposited films. The thickness was confirmed to be ≈200 nm for all prepared thin films. The dispersion of the real and imaginary part of refractive index for the as-deposited $Ge_8Sb_{2-x}Bi_xTe_{11}$ thin films prepared by the PLD or FE technique is shown in Fig. 4. The n and the k values obtained for PLD films (black lines) are larger than those for the FE thin films (red lines). The larger refractive index of PLD films in comparison with FE films can be explained by their higher density. The refractive index increases with the increasing Bi content in the $Ge_8Sb_{2-x}Bi_xTe_{11}$ films which can be related to the higher polarizability of Bi in comparison with Sb assuming the validity of the Clausius-Mossotti relation [45, 46].

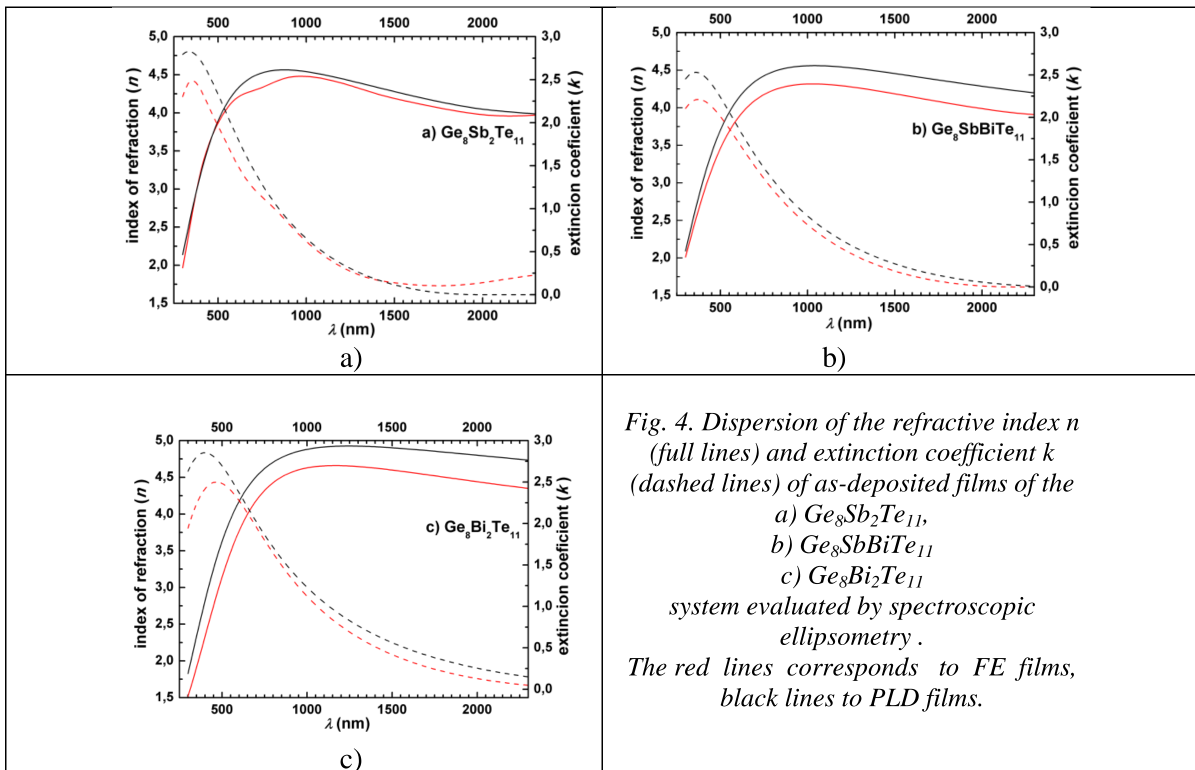

Fig. 4. Dispersion of the refractive index n (full lines) and extinction coefficient k (dashed lines) of as-deposited films of the a) $Ge_8Sb_2Te_{11}$, b) $Ge_8SbBiTe_{11}$ c) $Ge_8Bi_2Te_{11}$ system evaluated by spectroscopic ellipsometry . The red lines corresponds to FE films, black lines to PLD films.

By using a UV/Vis/NIR spectrophotometer, the spectral dependence of optical reflectivity for amorphous and crystalline thin films was measured. From the reflectivity data the optical contrast *C* [47] was determined (Tab.4). The values of optical contrast *C* of the prepared films are given by equation

$$C = (R_c - R_a)/R_c \cdot 100\% \quad (2)$$

where R_c is the reflectivity of crystalline film and R_a is the reflectivity of amorphous film. The reflectance values were typically between 20 and 41 % for the most samples and wavelengths. The optical contrast for the studied materials was at least 20 %, which is relatively high value for optical recording.

Table 4. Optical contrast C at the given wavelengths $Ge_8Sb_{2-x}Bi_xTe_{11}$ composition

Thin films	Method	λ=405 nm	λ=650 nm	λ=780 nm
		C (%)		
$Ge_8Bi_2Te_{11}$	FE	40	36	34
	PLD	25	30	30
$Ge_8SbBiTe_{11}$	FE	37	36	30
	PLD	35	33	20
$Ge_8Sb_2Te_{11}$	FE	28	38	40
	PLD	30	38	41

4. Conclusions

$Ge_8Sb_{2-x}Bi_xTe_{11}$ amorphous thin films (where x= 0; 1; 2) were deposited by the Flash Thermal Evaporation (FE) and Pulsed Laser Deposition (PLD) from the bulk samples, which were synthesized by the melt-quenching technique. XRD analysis confirmed that the amorphous films crystallize upon the heat treatment into the cubic phase and with increase Bi content in the rhombohedral and hexagonal phase, respectively. From DSC results it was found that the temperature of the crystallization and also the activation energies of crystallization decreased with increasing concentration of Bi.

The difference in electrical sheet resistance between the amorphous and crystalline states, was almost by 3-4 orders of magnitude. Therefore, from the presented results it can be said that higher Bi the concentration reduces temperature and activation energy the phase transition. Moreover, the studied materials exhibit a large difference in thermal, electrical and optical properties between the amorphous and crystalline state. The high optical contrast make the studied samples promising for PRAM memories.

Acknowledgements

This work was supported by the project CZ.1.05/4.1.00/11.0251 Center of Materials and Nanotechnologies from the Czech Ministry of Education, Youth and Sports of the Czech Republic. We would like to thank Lukas Strizik for the measuremend of variable angle spectroscopic ellipsometry.

References

[1] S. R. Ovshinsky, Phys. Rev. Lett., **21**, 1450 (1968).
[2] N. Yamada, E. Ohno, K. Nishiuchi, N. Akahira, M. Takao, J. Appl. Phys., **69**, 2849 (1991).
[3] M. Chen, K. A. Rubin and R. W. Barton, Appl. Phys. Lett., **49**, 502 (1986).
[4] N. Yamada, M. Takao, and M. Takenaga, Proc. SPIE, **695**, 79 (1986).

[5] E. Ohno, N. Yamada, T. Kurumizawa, K. Kimura, M. Takao, J. Appl. Phys., **28**, 1235 (1989).
[6] S. Kuypers, G. Van Tendeloo, J. Van Landuyt, and S. Amelinckx, J. Solid State Chem. **76**, 108 (1988).
[7] G. R. Gurbanov, Russian Journal of Inorganic Chemistry, **58**, 91 (2013).
[8] E. Prokhorov, J. J. Gervacio-Arciniega, G. Luna-Bárcenas. Y. Kolvalenko, F. J. Espinoza-Beltrán, and G. Trápaga, J. Appl. Phys., **113**, 113705 (2013).
[9] S. Kozyukhin, A. Sherchenkov, A. Babich, P. Lazarenko, H. P. Nguyen, and O. Prikhodko, Can. J. Phys., **92**, 684 (2014).
[10] B. Zhang, W. Zhang, Z. Shen, Y. Chen, J. Li, S. Zhang, Z. Zhang, M.s Wuttig, R. Mazzarello, E. Ma, and X. Han, Appl. Phys. Lett., **108**, 191902 (2016).
[11] K. A. Kokh, V. V. Atuchin, T. A. Gavrilova, N. V. Kuratieva, N. V. Pervukhina, N. V. Surovtsev, Solid State Communications, **177**, 16 (2014).
[12] L. E. Shelimova, O. G. Karpinskii, M. A. Kretova, V. I. Kosyakov, V. A. Shestakov, V. S. Zemskov, F. A. Kuznetsov, Inorganic Mater., **36**, 768 (2000).
[13] Y. Kim, X. Chen, Z. Wang, J. Shi, I. Miotkowski, Y. P. Chen, P. A. Sharma, A. L. Lima Sharma, M. A. Hekmaty, Z. Jiang, and D. Smirnov, Appl. Phys. Lett. **100**, 071907 (2012).
[14] M. Krbal, A. V. Kolobov, J. Haines, P. Fons, C. Levelut, R. L. Parc, M. Hanand, J. Tominaga, A. Pradel, M. Ribes, Phys. Rev. Lett. **103**, 115502 (2009).
[15] M. Hase, P. Fons, K. V. Motrofanov, A.V. Kolobov and J. Tominaga, Nat. Commun. **6**, 8367 (2015).
[16] M. Frumar, B. Frumarova, T. Wagner, M. Hrdlicka, J. Mater. Sci: Mater Electron **18**, S169 (2007).
[17] L. E. Shelomova, O. G. Karpinsky, M. A. kretova, E. S. Avilov, Journal of Alloys and Compounds, **243**, 197 (1996).
[18] Su-Shia Lin, Mater. Sci. Eng., **B 129**, 116 (2006).
[19] A. Kolobov, P. Fons, A. Frenkel, A. Ankudinov, J. Tominaga, and T. Uruga, Nat. Mater. **3**, 703 (2004).
[20] M. Krbal, A. V. Kolobov, P. Fons, K. V. Mitrofanov, Y. Tamenori, J. Hegeduus,S. R. Elliott, J. Tominaga, Appl. Phys. Lett. **102**, 111904 (2013).
[21] J. Hegedüs and S. Elliott, Nat. Mater. **7**, 399 (2008).
[22] D. Loke, T. H. Lee, W. J. Wang, L. P. Shi, R. Zhao, Y. C. Yeo, T. C. Chong, and S. R. Elliott, Science **336**, 1566 (2012).
[23] A. V. Kolobov, M. Krbal, P. Fons, J. Tominaga and T. Uruga, Nat. Chem., (2011).
[24] M. Krbal, A. Kolobov, P. Fons, J. Tominaga, S. Elliott, A. Guissani, R. Perumal, K. Calarco, T. Matsunaga, N. Yamada, K. Nitta et al., Phys. Rev. **B 86**, 045212 (2012).
[25] K. Shportko, S. Kremers, M. Woda, D. Lencer, J. Robertson, and M. Wuttig, Nat. Mater. **7**, 653 (2008).
[26] K. Shimakawa, L. Strizik, T. Wagner, and M. Frumar, Apl. Mater. **3**, 041801 (2015).
[27] S. Buller, C. Koch, W. Bensch, P. Zalden, R. Sittner, S. Kremers, M. Wuttig, U. Schürmann, L. Kienle, T. Leichweiß, J. Janek, Chem. Mater., **24**, 3582 (2012).
[28] T. Matsunaga, H. Morita, R. Kojima, N. Yamada, K. Kifune, Y. Kubota, Y. Tabata, J.-J. Kim, M. Kobata, E. Ikenaga, et al., J. Appl. Phys. **103**, 093511 (2008).
[29] M. Krbal, A. V. Kolobov, P. Fons, R. E. Simpson, T. Matsunaga, J. Tominaga, N. Yamada, Phys. Rev. **B 84**, 104106 (2011).
[30] A. Sherchenkov, S. Kozyukhin, A. Babich, J. Therm. Anal. Calorim., **117**, 1509 (2014).
[31] P. I. Lazarenko, A. A. Sherchenko, S. A. Kozyukhin, M. Y. Shtern, S. P. timosenkov, D. G. Gromov, E. N. Redichev, Proc. SPIE, 944006 (2014).
[32] T. Wagner, J. Orava, J. Prikryl, T. Kohoutek, M. Bartos, M. Frumar, Thin Solid Films **517**, 4694 (2009).
[33] M. Frumar, B. Frumarova, P. Nemec, T. Wagner, J. Jedelsky, M. Hrdlicka, J. Non Cryst. Solid. **352**, 544 (2006).
[34] P. Nemec, J. Prikryl, V. Nazabal, and M. Frumar, J. Appl. Phys. **109**, 073520 (2011)
[35] H. E. Kissinger, Anal. Chem., **29**, 1702 (1957).
[36] J. Prikryl, M. Hrdlicka, M. Frumar, J. Orava, L. Benes, M. Vlcek, P. Kostal, L. Hromadko,

T. Wagner, J. Non Cryst. Solid., **355**, 1998 (2009).
[37] H. Fujiwara, Spectroscopic Ellipsometry: Principles and Applications, John Wiley & Sons Ltd., Sussex, England, 2007.
[38] O. G. Karpinsky, L. E. Shelimova, M. A. Kretova, J.-P. Fleurial, J. of Alloys and Compounds, **265**, 170, (1998).
[39] Y. Liang, W. Wang, B. Zeng, G. Zhang, J. Huang, J. Li, T. Li, Y. Song, X. Zang, Journal of Alloys and Compounds, **509**, 5147 (2011).
[40] Z. Yu, X. Wang, Y. Du, S. Aminorroaya-Yamni, C. Zhang, K. Chuang, S. Li, Journal of Crystal Growth, **362**, 247 (2013).
[41] L. E. Shelimova, O. G. Karpinskii, V. I. Kosyakov, V. A. Shestakov, V. S. Zemskov, and F. A. Kuznetsov, Journal of Structural Chemistry, **41**, 81 (2000).
[42] R. Svoboda, V. Karabyn, J. Málek, M. Frumar, L. Beneš, M. Vlček, J. of Alloys and Compounds, **674**, 63 (2016).
[43] N. F. Mott, E. A. Davis, Electronic Processes in Non-Crystalline Materials, Oxford Clarendon Press; London, 1971.
[44] K. Shimakawa, T. Wagner, M. Frumar, F. Kadlec, Ch. Kadlec and S. Kasap, J. Appl. Phys.**114**, 233105-1 (2013).
[45] R. Clausius, Die Mechanische Wärmlehre, **Vol. II.**, 1879.
[46] O. Mossotti, Mem. E Fisica di Modena, **24**, 49 (1850).
[47] F. Gan, L. Hou, G. Wang, H. Liu, J. Li, Mater. Sci. Eng., **B76**, 63 (2000).